# Estimating Drivers Cell State Transitions using Gene Regulatory Network Models

Daniel Schlauch[1] and Kimberly Glass[2,3] John Quackenbush[1,3]

[1]Department of Biostatistics and Computational Biology,
Dana-Farber Cancer Institute and Department of Biostatistics,
Harvard TH Chan School of Public Health, Boston, MA 02215
[2]Channing Division of Network Medicine, Brigham and Women's
Hospital, Boston, MA 20015
[3]Department of Medicine, Harvard Medical School, Boston, MA
20015

December 22, 2015

**Abstract**

In the language of systems biology, the state of a cell can be represented by a gene regulatory network that characterizes the gene transcriptional processes that are active in that cell type. And transitions that occur in a wide range of biological processes, ranging from development to disease, can be thought of as transformation of the gene regulatory network from its initial state to its final state. Here we propose a regression-based generalization of the PANDA method for gene regulatory network inference for individual states, and a linear algebra approach to modeling cell state transitions, identifying transcription factors that alter the network structure as cell states change.

## The problem of gene regulatory network inference

One of the fundamental problems is biology is modeling the transition between biological states such as that which occurs during development or as a healthy tissue transforms into a disease state. While it is appealing to conceive of this process as deterministic, reflecting a change from one well-defined phenotype to another, in truth the situation is much more complex. Neither the initial nor the final phenotype is discrete, but each falls into a continuum of states, which, on average, captures features of that phenotype. Indeed, within each tissue there are many, many cells, each of which is its own particular instance of that tissue—with unique patterns of gene expression and individual regulatory

processes. The same is true when considering individuals as each healthy and disease state is unique to each member of a study population. One way to conceptualize the state transition problem is to imagine that each phenotype has a characteristic gene regulatory network and that there are a set of processes that are either activated or inactivated to transform the network in the initial state into that characterizing the final state. Identifying those changes could, in principle, help us to understand not only the processes that drive the state change, but also how one might intervene to either promote or inhibit such a transition.

As our ability to generate large-scale, integrative multi-omic datasets has grown, there has been an increased interest in using those data to infer gene regulatory networks to model fundamental biological processes. While there have been many network inference methods published, each of which uses a different approach to estimating the "strength" of interactions between genes (or between transcription factors and their targets), they all suffer from the same fundamental limitation. Every method relies on estimating weights that represent the likelihood of an interaction between two genes and then setting a threshold to identify "real" (high confidence) edges. While setting edge confidence thresholds allows us to graphically represent networks and allows us to compare networks based on the presence or absence of edges, it ultimately requires that we discard information regarding those "weak" edges that fail to reach significance. Now, one could argue that discarding low significance edges is sensible as one common goal in network inference is to deduce a single, high confidence network model that represents a particular phenotype under study or, in some cases, a transition between phenotypes. An alternative view is that these edges contain estimates for gene coexpression that may be muted due to the heterogeneity of the biological sample and that networks are best described by edgeweights on a continuous scale. Furthermore, we argue that the inclusion of all network edgeweights in downstream analyses allows for the collection of systematic, though subtle, differences in coexpression which may otherwise have been washed out by extraneous noise.

## BERE: A regression-based approach to modeling gene regulatory networks

In 2013, we described PANDA [3], a method [11] for estimating gene regulatory networks that uses "message passing"ă [2] to integrate multiple types of genomic data. PANDA begins with a prior regulatory network based on mapping transcription factor motifs to a reference genome and integrates other sources of data, such as protein-protein interaction and gene expression profiles, to estimate individual sample networks. While PANDA has proven to be very useful in a number of applications [4, 5, 8], its iterative approach to edge-weight optimization limits its utility in situations requiring a large number of network bootstrap estimations. To address this limitation, we developed BERE, Bi-

partite Edge Reconstruction from Expression. BERE approaches the network inference problem by considering the available evidence of an edge for each possible TF-gene pair. This evidence can be divided into two components, referred to here as direct and indirect. Consider the edge between a TF and a gene, referred to here as $TF_i$ and $g_j$, respectively. The direct evidence, $d_{i,j}$, consists of the squared conditional correlation of the $g_i$ and $g_j$ given all other regulators of $g_i$. Where $g_i$ is the gene which encodes $TF_i$

$$d_{i,j} = cor\left(g_i, g_j \mid \{g_{k,-j} : k \neq j, k \in \mathbf{TF}\}\right)^2$$

Naturally, the use of direct evidence inadequately captures regulatory relationships due to the impacts of technical noise and numerous biological external factors such as stable or transient protein-protein interactions, post-translational modifications, etc. which may confound or modify a regulatory effect. These sources of confounding and variability in the expression pattern of a gene coding a TF may obscure the effects it has on all of its target genes. Therefore it is of value if we can complement our estimate of the likelihood of a regulatory mechanism by aggregating the information from the gene expression patterns of all suspected targets of transcription factors. PANDA achieves its superior performance in part by convergence towards "agreement", whereby large collections of gene expression patterns must agree with the proposed regulatory structure in order to claim an interaction. Similarly, BERE looks for agreement between the gene expression patterns of large sets of co-targeted genes. We refer to this feature as indirect evidence and can achieve this by again utilizing our set of regulatory priors. In this portion of the analysis we suspend the recognition of a TF as a member of the gene list and instead consider each of the m TFs to be binary classifications across the entire gene list. Class labels are determined by the presence or absence of a sequence binding motif for that TF in the vicinity of the gene.

The indirect evidence between the two nodes, $e_{i,j}$, represents the fitted probability that $g_i$ belongs to the class of genes targeted by $TF_j$. $g_i$ is considered to be a new observation placed into the $n-$dimensional space separated by transcription factor targets and non-targets. To divide up the space, BERE uses a regularized logistic regression on the gene expression data with the training set taken to be all genes and the training labels taken to be the existence or non-existence of a known sequence motif for $TF_j$ upstream of $g_i$. The penalized model matrix comes from the recognition that correlations between co-regulated genes will be most strong when the $TF_j$ is most prevalent. We therefore use the abundance of $TF_j$ to weight the penalized model matrix, providing increased sensitivity for detecting coexpression for those samples in which we most expect it to occur. To build each of our classifiers we use the $L2$ regularization with the penalized model matrix, $\mathbf{Q}$, a diagonal matrix with weights equal to the the inverse expression value of the transcription factor. Effectively, we maximize the penalized logistic likelihood function

$$\sum_{i=1}^{n} log\left[exp\left(\beta' \mathbf{x_i}\right)^{Y_i} \left\{1 - exp\left(\beta' \mathbf{x_i}\right)\right\}^{1-Y_i}\right] - \lambda \beta' \mathbf{Q} \beta$$

3

This computation is run using the R package "penalized", with the penalty term lambda estimated via default 5 fold cross validation.

By scoring each gene according to the strength of indirect evidence for a regulatory response to each of the TFs, we can combine this with the direct evidence of regulation (squared conditional correlation of expression for genei and $TF_i$). The appropriate manner in which to combine direct and indirect evidence remains an open question. Though both measures are bounded by [0,1] their interpretation is quite different. The direct evidence can be considered in terms of it's conditional gene expression $R^2$ between nodes, while the indirect evidence is interpreted as a probability. We use a non-parametric approach to combine evidence. The targets of each TF are then ranked and combined as a weighted sum, $w_i = (1 - \alpha)\left[rank\left(d_i\right)\right] + \alpha\left[rank\left(e_i\right)\right], i \in \{1, \ldots, n\}$. Our choice of the weight, $\alpha$, here is based on empirical evaluation, and perhaps not surprisingly, is loosely correlated with organism complexity. In validation sets from Yeast, the optimal alpha was observed near $\alpha = .9$ while simpler E. coli datasets saw an optimal value of $\alpha = .6$ and an in silico dataset, optimality was achieved at $\alpha < .5$ This naturally reflects the fact that the increased complexity of the network necessitates the use of larger scale agreement between genes, rather than a reliance on pairwise correlations between potentially noisier and more complex expression patterns.

# Modeling cell state transitions as a problem in gene regulatory network transition

Cell state transitions—such as those that occur during development, or as healthy tissue transforms into a disease phenotype—are fundamental properties of biological systems. Understanding what drives these transitions, and modeling the processes, is one of the great open challenges in modern biology. One way to conceptualize the state transition problem is to imagine that each phenotype has its own characteristic gene regulatory network, and that there are a set of processes that are either activated or inactivated to transform the network in the initial state into that which characterizes the final state. Identifying those changes could, in principle, help us to understand not only the processes that drive the state change, but also how one might intervene to either promote or inhibit such a transition. The starting point for modeling cell state transitions is to model the initial and final cell states. One might imagine that the initial and final cell states consist of characteristic processes, some of which are shared (sometimes referred to as "housekeeping" functions) and others which are unique to the particular state. The way we understand these processes is that they are controlled by gene regulatory networks in which transcription factors (and other regulators) moderate the transcription of individual genes whose expression characterizes the state. One way to represent such processes is to draw a directed network graph, in which transcription factors and genes are nodes network in the network, and edges represent the regulatory interac-

tions between transcription factors and their target genes that are active in, and characteristic of, a particular cellular state. One way of representing such a network, with interactions between m transcription factors and n target genes, is as a binary $m \times n$ "adjacency matrix," with 1's representing active transcription factor-target interactions, and 0's representing the lack of a transcription factor-target gene regulatory interaction. One can then think of a cell fate transition as the process that transforms the network in its initial state to its final state form, adding and deleting edges to remake the network that characterizes one phenotype into that which characterizes the other. Using the adjacency matrix formalism, one can think of this as a problem in linear algebra in which we attempt to find an $m \times m$ "transition matrix" $\mathbf{T}$, subject to a set of constraints that approximates the conversion from the initial network's adjacency matrix $\mathbf{A}$ into the final network's adjacency matrix $\mathbf{B}$, or
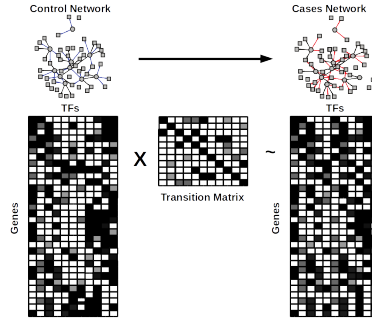
$$\mathbf{B} = \mathbf{AT}$$



Figure 1: **Overview of the Transition Matrix problem.** Our approach seeks to find the $TF \times TF$ matrix which best characterizes the transition in TF targetting between cases and controls. We can think about this problem as the estimation of the set of TF-TF interactions which minimizes edgeweight error in the cases network when applied to the controls network.

While it is appealing to conceive of this process as deterministic, reflecting a change from one well-defined phenotype to another, in truth the situation is much more complex. Neither the initial nor the final phenotype is discrete, but each falls into a continuum of states, which, on average, captures the features of that phenotype. Indeed, within each tissue there are many, many cells, each of which is its own particular instance of that tissue—with unique patterns of gene expression and individual regulatory processes. In the language of adjacency matrices, what this means is that rather than representing each state by a matrix with binary entries, what one should do is use a representation in which entries are continuous, representing the strength of the transcription factor-target gene interaction averaged over the collection of samples (or cells) representing each state. And consequently, the problem of estimating the transition matrix is

generalized to solving , where E is an $m \times n$ error matrix representing the uncertainty in the estimation of the individual edges. In this formalism, modeling the cell state transition is equivalent to estimating the appropriate transition matrix T that maps how the transcription factor-target gene interactions are "rewired" between states. And one could hypothesize that the drivers of the cell state transition are those transcription factors that are have the greatest change in the targets that they regulate. In evaluating the state transitions, we recognize the limitations of current network inference methods to predict individual edgeweights. It's therefore of interest to combine measurements across sets of edgeweights in order to extract meaningful signal from a network perturbation. Effectively, we approached the problem as a dimension reduction problem with the goal of identifying high-influence systematic regulatory network alterations rather than isolated independent events. There are many existing methods for reducing a high-dimensional matrix such as a gene regulatory adjacency matrix. Commonly, Principal Components Analysis (PCA) identifies eigenvectors which can reconstruct the greatest degree of variance from the original data. One drawback of this approach is the lack of interpret-ability of these vectors. Our transition matrix approach can be considered as a data reduction method which (1) preserves the intuitive interpretation of its vectors and (2) utilizes our expectation that meaningful network transitions will occur via biologically systematic alterations and not via random, independent edge alterations.

## TM significantly improves TF-TF edge estimation from simulated gene expression data

To evaluate the ability of our method to recover edges between transcription factors, we generated simulated gene expression data. We began by generating a true controls adjacency matrix, $M_{0(p \times q)}$, describing the weighted edges between $q$ transcription factors and $p$ genes. A state transition was generated by sampling 100 TF-TF pairs and adjusting the edgeweight at the corresponding point on the true cases adjacency matrix, $M_{1(p \times q)}$. These TF-TF pairs ultimately represent the edges that we seek to recover and the size of the adjustments are the parameters of interest. We sampled from a multivariate Gaussian distribution with the off-diagonal of the variance-covariance matrix, $\Sigma$, defined as the $M_0 M_0'$. Furthermore, we scaled the magnitude of the diagonal of $\Sigma$ to achieve the desired proportion of noise. We aimed for an area under the curve of the receiver-operator characteristic of approximately 0.70 as this has reasonably been achieved in existing biological studies [3].

This sampling represented our simulated control samples. The adjusted adjacency matrix, $M_1$, was similarly used to generate simulated expression data for the cases group. Next, we reconstructed the networks from our expression data using a set of commonly used network inference methods - Weighted Gene Correlation Network Analysis (WGCNA) [6] [7], Topological Overlap Measure (TOM) [13], Algorithm for the Reconstruction of Gene Regulatory Net-

6

AUC-ROC for Eedgeweight differences vs Transition Matrix using various NI methods

| NI Method | Networks | Edgeweight differences | Transition Matrix |
|---|---|---|---|
| Pearson | .701 (p<.0001) | .510 (p=.72) | .802 (p<.0001) |
| WGCNA(6) | .701 (p<.0001) | .512 (p=.61) | .688 (p<.0001) |
| WGCNA(12) | .701 (p<.0001) | .52 (p=.10) | .589 (p=.02) |
| ARACNE | .515 (p<.0001) | .523 (p=.58) | .566 (p=.09) |
| CLR | .691 (p<.0001) | .57 (p=.19) | .814 (p<.0001) |
| TOM | .700 (p<.0001) | .51 (p=.62) | .689 (p<.0001) |
| PANDA*(Motif=.570) | .740 (p<.0001) | .520 (p=.13) | .793 (p<.0001) |
| PANDA** (Motif=.547) | .676 (p<.0001) | .509 (p=.43) | .66 (p<.0001) |

Table 1: **Comparison of edgeweight difference to Transition Matrix in simulated case-control gene expression**. Several network inference methods were run on our *in silico* case-control data. The overall network area under the curve of the receiver-operator characteristic (AUC-ROC) was performed for each method averaged across cases and controls. For PANDA* and PANDA**, which additionally utilizes motif prior information, motif priors with AUC-ROC of .570 and .547 were used. The naive TF-TF transitions were calculated as the difference in TF-TF edgeweight between cases and controls. The transition matrix TF-TF transitions used the absolute transition matrix values.

works (ARACNE) [10], Context Likelihood of Relatedness (CLR) [1], Passing Attributes between Networks for Data Assimilation (PANDA) [3] and simple Pearson correlation (PC).

We applied the transition matrix with default parameters on each case-control pair of networks. For comparison, we estimated the difference from case to control in edgeweights derived from the direct edge prediction using each network inference method. The predictions for the TM approach and the direct approach were evaluated by the area-under-the-curve of the receiver-operator-characteristic (AUCROC) with the true transition adjustments taken as the gold standard. For each of the network inference methods tested, we found substantial improvement in the predicted transitions over the direct network inference method. In many cases, the edgeweight difference (column 2) was not statistically significant for predicting transitions, but when the TM was applied (column 3) a strong predictive signal appeared. In other cases, an existing signal was observed using the direct approach, but was dramatically improved with the application of the TM.

The intuition behind the improvement is simple. While the estimation of a TF-TF edge is typically evaluated via some pairwise gene expression pattern which may be rife with technical and biological noise, the TM approach borrows information from all downstream targets in estimating the relative change in relationship between the TFs.

# Transition Matrix Analysis

Many mechanisms which may be differentially present, such as RNA degredation, post-translational modification, protein-level interactions and epigenetic alterations have the ability to impact downstream targeting without impacting the expression level of the TF itself. It may be of particular scientific or therapeutic interest to identify those TFs which have undergone significant overall changes in behavior between controls and cases. With that objective in mind, we express the statistic- differential Transcription Factor Involvement (DTFI), as a measure for quantifying this property.

$$s_j = \frac{\sum_{i=1}^{m} I\left(i \neq j\right) \tau_{i,j}^2}{\sum_{i=1}^{m} \tau_{i,j}^2}$$

DTFI can be loosely interpreted as the proportion of TF targeting patterns which is explained by the targeting patterns of other available TFs. This measure, a statistic on the interval $[0,1]$ seeks to elucidate transitions which are systematic, informative, and non-arbitrary in nature by capturing only the edgeweight signal for which there is an attributable regulatory pattern. The distribution of this statistic under the null has a mean and standard deviation which depend on the motif structure. In particular, both mean and standard deviation are increased for TFs which have fewer prior regulatory targets. From a statistical perspective, TFs with relatively more targets are able to generate more stable targeted expression patterns, which leads to more consistent estimates in "agreement" algorithms such as PANDA and BERE. From a biological perspective, increased motif presence may indicate that the TFs are more likely to be ubiquitous housekeeping proteins that do not meaningfully alter their involvement between cases and controls. The dependence of the null distribution on the motif structure is addressed via the following resampling procedure.

1. Gene expression samples are randomly assigned to case and control forming the null-case and null-control with group sizes preserved.

2. GRNs are reconstructed for the null-case and null-control with the same prior regulatory structure.

3. The transition matrix algorithm is applied for the two null networks.

4. The differential TFI is calculated for each TF.

5. Repeat 1-4 1000 times.

# Transition Matrix finds concordance in independent datasets for COPD

We applied our method to three case-control datasets for Chronic Obstructive Pulmonary Disease (COPD)- Evaluation of COPD Longitudinally to Identify
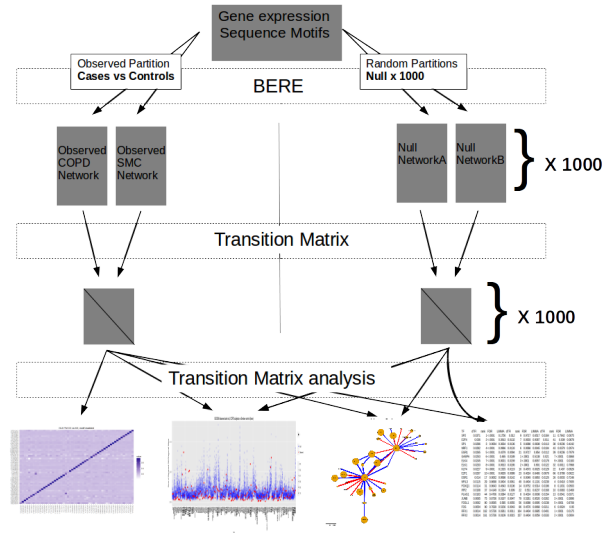
Figure 2: **Overview of Transition Matrix analysis workflow.** (1) BERE is applied separately to subsets of the gene expression data including the cases group, the controls group and 1000 permutations of the cases and controls labels. (2) Transition matrix is estimated between the cases and controls and each of the pair or permuted "cases" and "controls".

Predictive Surrogate Endpoints (ECLIPSE), the COPDGene study, and Lung Genomics Research Consortium (LGRC). Each of these studies consisted of gene expression assays obtained from patients with COPD and a set of smoker controls. The tissue used in the ECLIPSE and COPDGene study was peripheral blood mononuclear cell (PBMC), while lung tissue was sampled for LGRC. It is therefore unsurprising that agreement is more strongly achieved in the former studies compared to the latter. However it is quite notable that the we do see much of the same dTFI signal across studies involving different tissue types.

We separately applied our BERE network inference approach on cases and controls and computed the transition matrix. Top significance hits for dTFI showed strong concordance between each of the datasets. Out of 166 TF used in this study, seven were among top 10 most differentially involved in both the ECLIPSE and COPDGene studies. Furthermore, three of these seven TFs (GABPA, ELK4, ELK1) also appeared as significant in the LGRC results with FDR<.01.

Overall, there was a strong correlation between results in the two PBMC studies $\left(R^2 = 0.82\right)$, and a weak correlation between cross-tissue results for LGRC-ECLIPSE $\left(R^2 = 0.33\right)$ and LGRC-COPDGene$\left(R^2 = 0.39\right)$.
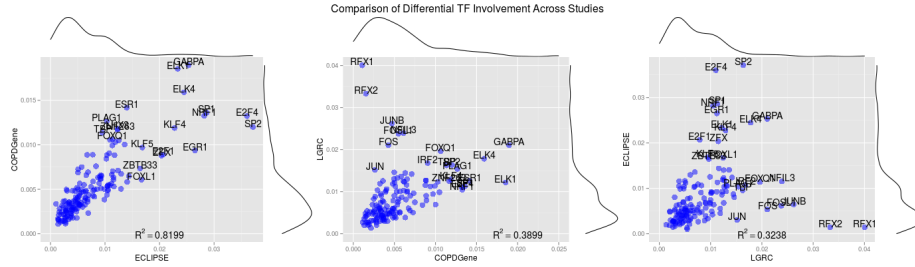


Figure 3: Comparison of dTFI for 166 TFs across three independent studies. Results for two studies with gene expression data obtained from PBMC (ECLIPSE and COPGene) show strong concordance with a high degree of agreement, particularly for top hits. Both of these studies are less consistent with the LGRC, but contain several significant TFs in agreement with the other studies.

Of further interest is the particular TFs which are differentially observed across studies. For example, ERS1, the gene encoding Estrogen receptor alpha (ES-$\alpha$) is likely to behave differently in males compared with females. We found that this TF is significantly differentially involved in the COPDGene study - identified as the $4th$ most differentially involved TF, but not the ECLIPSE study. Accordingly, the COPDGene study had a greater gender disparity (Odds Ratio = 1.126) than the ECLIPSE study (Odds Ratio = 1.067).

Notably in the LGRC dataset, we discovered a differential targetting pattern involving the TFs RFX1 and RFX2. Both of these transcription factors were highly statistically significant (FDR<.0001) and ranked as the top two results in the LGRC study. However, their signal was muted in the ECLIPSE and COPDGene studies, neither of which identified these transcription factors as

| | ECLIPSE | | | | COPDGene | | | | LGRC | | | |
|---|---|---|---|---|---|---|---|---|---|---|---|---|
| TF | dTFI | rank | FDR | LIMMA | dTFI | rank | FDR | LIMMA | dTFI | rank | FDR | LIMMA |
| SP2 | .0371 | 1 | <.0001 | .1756 | .0120 | 9 | .9717 | .6517 | .0164 | 11 | .7642 | .0075 |
| E2F4 | .0360 | 2 | <.0001 | .3913 | .0132 | 7 | .0003 | .9367 | .0110 | 41 | .039 | .0878 |
| SP1 | .0286 | 3 | .0004 | .3634 | .0136 | 5 | .6088 | .0838 | .0113 | 38 | .9236 | .4242 |
| NRF1 | .0282 | 4 | <.0001 | .0966 | .0133 | 6 | .0068 | .0045 | .0104 | 43 | .0379 | .2974 |
| EGR1 | .0265 | 5 | <.0001 | .4379 | .0094 | 21 | .9717 | .8540 | .0112 | 39 | .9236 | .7979 |
| GABPA | .0253 | 6 | <.0001 | .4650 | .0189 | 1 | <.0001 | .5138 | .0210 | 7 | <.0001 | .3868 |
| ELK4 | .0245 | 7 | <.0001 | .0001 | .0159 | 3 | <.0001 | .8057 | .0178 | 9 | <.0001 | .0183 |
| ELK1 | .0233 | 8 | <.0001 | .0913 | .0185 | 2 | <.0001 | .9010 | .0122 | 32 | .0011 | .7968 |
| KLF4 | .0227 | 9 | <.0001 | .1915 | .0119 | 10 | .4573 | .0025 | .0129 | 22 | .437 | .0526 |
| E2F1 | .0207 | 10 | <.0001 | .6929 | .0089 | 23 | .4024 | .6465 | .0079 | 66 | .3789 | .0022 |
| ESR1 | .0140 | 17 | .0002 | .9598 | .0142 | 4 | .0049 | .5853 | .0125 | 26 | .0033 | .7246 |
| NFIL3 | .0115 | 29 | .8698 | .0404 | .0061 | 49 | .4404 | .1191 | .0239 | 4 | .0418 | .7605 |
| FOXQ1 | .0114 | 31 | .9643 | .4543 | .0106 | 14 | .9752 | .5314 | .0196 | 8 | .1031 | .0503 |
| IRF2 | .0108 | 37 | .4149 | .1914 | .0090 | 22 | .531 | .8237 | .0168 | 10 | .0083 | .2469 |
| PLAG1 | .0103 | 44 | .4706 | .0384 | .0127 | 8 | .4024 | .0008 | .0154 | 13 | .0541 | .0371 |
| JUNB | .0065 | 75 | .8736 | .0197 | .0047 | 79 | .5281 | .9526 | .0262 | 3 | <.0001 | .3996 |
| FOSL1 | .0062 | 80 | .8595 | .5850 | .0055 | 56 | .6088 | .6995 | .0238 | 5 | <.0001 | .8708 |
| FOS | .0054 | 90 | .7639 | .5156 | .0043 | 86 | .4576 | .6668 | .0211 | 6 | .0024 | .9500 |
| RFX1 | .0014 | 162 | .5736 | .0361 | .0011 | 164 | .4404 | .0885 | .0401 | 1 | <.0001 | .0175 |
| RFX2 | .0014 | 161 | .5736 | .0109 | .0015 | 157 | .4404 | .0059 | .0333 | 2 | <.0001 | .0004 |

Table 2: Combined list of TFs which were among the top 10 hits (out of 166 available TFs) in any of the 3 studies, ordered by the dTFI in the ECLIPSE study. For each study, columns indicate the TF's (1) differential TF Involvement, (2) dTFI Rank within list of TFs, (3) Significance of dTFI by false discovery rate, and (4) p-value for LIMMA differential gene expression analysis.

drivers of the Smoker Control to COPD transition. There are many possible explanations for this result, but it is reasonable to speculate that the dramatically different result is due to the fact that the tissue of origin for the LGRC differs from the ECLIPSE and COPDGene tissue.

The top hits which are most consistent across studies have been implicated in independent studies for the development of COPD.

Two of the top 3 hits, NRF1 and GABPA have been implicated in a mitochondrial mechanism for disease progression [Cloonan, Suzanne M et al]. Interestingly, the majority of the TFs identified as differentially involved do not exhibit significant differential gene expression. This suggests that for these proteins, their role in the disease may not occur until the post-transcription stage. It also suggests that conventional gene expression analysis is insufficient for identifying many of the TF drivers of disease.

# Supplement

## Transition matrix finds significant protein-protein interaction

As noted above, there are numerous biological regulatory mechanisms which may yield detectable transitions. Of particular interest are those which are less

readily detectable via conventional methods, such as differential gene expression analysis. One mechanism studied here involves one TF binding to another TF to promote, suppress or alter one or both of their regulatory patterns. These multiprotein interactions create combinatorial complexity that can explain much of the variation in organism complexity which is unexplained by number of genes alone [9].

To test the ability to detect protein level interactions, we compared our estimated transitions to a set of known protein-protein interactions [12]. This set contained 223 pairwise interactions between a total of 189 transcription factors. Of interest was the effectiveness of identifying these interactions via the transition from one phenotypic state to another. This is a challenging task for several reasons, (1) protein-protein interaction is merely one of a myraid of detectable transition mechanisms, (2) it is reasonable to assume that only a small subset of the known PPI are actually differentially present between case and control and (3) technological limitations in the active field of proteomics cannot be expected to identify all interactions with a reasonable degree of certainty.

For the transition from Smoker control to COPD, we compared for the transition estimates to those generated by the transition from randomly resampling the phenotypic labels. The AUCROC for the prediction of the 223 known protein-protein interactions was $0.5695$ ($p = 0.018$), suggesting that our approach is successful at detecting this highly obscured signal.

## Efficiency of estimation

Let $\mathbf{x}_p$ be a Gaussian $p$-vector representing a sample of gene expression data containing $q$ transcription factors and $p - q$ non-transcription factor genes.

$$\mathbf{x}_p \sim N\left(\mu, \Sigma\right)$$

where $\mu$ is the $p$-vector of mean gene expression values and $\Sigma$ is the $p \times p$ variance-covariance matrix. In this scenario, $\Sigma$ may be regarded as a combination of two independent variance-covariance sources- (1) biological signal, (2) biological noise and technical noise.

In investigating gene regulation, many network inference methods are constructed for the estimation of the $p \times q$ subset of $\Sigma$ pertaining to the effect of the $q$ TFs on the $p$ genes. In identifying drivers of state transitions, we seek to focus on the $q \times q$ matrix of TF-TF effects. We show that our method vastly ourperforms commonly used network inference methods in estimating these specific effects.

Consider a state change between two experimental conditions, A and B, characterized by an alteration of size $\delta$ to the biological signal component of the TF-TF variance-covariance matrix at point $\Sigma_{i,j}$ where $i$ and $j$ are indices for two TFs in $\Sigma$.

Using a univariate coexpression calculation (the basis for Pearson networks and WGCNA estimates), the estimated variance of our estimate of $\delta$ can be calculated:

12

$$-\rho_A < \delta < \rho_A, \delta + \rho_A \leq 1$$

$$
\begin{aligned}
Var\left(\hat{\rho}_{i,j,A} - \hat{\rho}_{i,j,B}\right) &= Var\left(\hat{\delta}_{cor}\right) \\
&\phantom{=} Var\left(\hat{\rho}_{i,j,A}\right) + Var\left(\hat{\rho}_{i,j,B}\right) \\
&= \frac{1-\rho_{i,j,A}^2}{n_A-2} + \frac{1-\rho_{i,j,B}^2}{n_B-2} \\
&= \frac{1}{n_A-2} + \frac{1}{n_B-2} - \frac{\rho_{i,j,A}^2}{n_A-2} - \frac{\rho_{i,j,B}^2}{n_B-2}
\end{aligned}
$$

Meanwhile, in condition B the new correlation of $TF_i$ with some gene, $gene_k$ $k \in 1,2\ldots p$ , denoted $cor^*$, becomes

$$cor^*\left(TF_i, gene_k\right) = cor\left(TF_i, gene_k\right) + \delta cor\left(TF_j, gene_k\right)$$

where the term $\delta cor\left(TF_j, gene_k\right)$ is the change due to the interaction of $TF_i$ and $TF_j$.

The variance of our estimate using the transition matrix can be expressed as follows:

$$
\begin{aligned}
Var\left(TM_{i,j}\right) &= Var\left(\hat{\delta}_{TM}\right) \\
&= \frac{\left(\frac{1}{p}\right)\sum_{k=1}^p vVar\left(\hat{\rho}_{i,k,A} - \hat{\rho}_{i,k,B}\right)}{\sum_{k=1}^p \left(\rho_{j,k} - \bar{\rho}_j\right)^2} \\
&= \frac{\left(\frac{1}{p}\right)\sum_{k=1}^p \left[Var\left(\hat{\rho}_{i,k,A}\right) + Var\left(\hat{\rho}_{i,k,B}\right)\right]}{\sum_{k=1}^p \left(\rho_{j,k} - \bar{\rho}_i\right)^2} \\
&\leq \frac{\left(\frac{1}{p}\right)\sum_{k=1}^p \left[\frac{1}{n_A-2} + \frac{1}{n_B-2}\right]}{\sum_{k=1}^p \left(\rho_{j,k} - \bar{\rho}_i\right)^2} \\
&\leq \frac{\frac{1}{n_A-2} + \frac{1}{n_B-2}}{\sum_{k=1}^p \left(\rho_{j,k} - \bar{\rho}_i\right)^2} \\
&\leq \frac{Var\left(\hat{\delta}_{cor}\right) + \frac{\rho_{i,j,A}^2}{n_A-2} + \frac{\rho_{i,j,B}^2}{n_B-2}}{\sum_{k=1}^p \left(\rho_{j,k} - \bar{\rho}_i\right)^2} \\
&\leq Var\left(\hat{\delta}_{cor}\right) + \frac{Var\left(\hat{\delta}_{cor}\right)\left(1 - \sum_{k=1}^p \left(\rho_{j,k} - \bar{\rho}_i\right)^2\right) + \frac{\rho_{i,j,A}^2}{n_A-2} + \frac{\rho_{i,j,B}^2}{n_B-2}}{\sum_{k=1}^p \left(\rho_{j,k} - \bar{\rho}_i\right)^2}
\end{aligned}
$$

So we have that $Var\left(TM_{i,j}\right) < Var\left(\hat{\delta}_{cor}\right)$ when

$$Var\left(\hat{\delta}_{cor}\right)\left(1 - \sum_{k=1}^p \left(\rho_{j,k} - \bar{\rho}_i\right)^2\right) < \frac{\rho_{i,j,A}^2}{n_A-2} + \frac{\rho_{i,j,B}^2}{n_B-2}$$

Since each term except $\left(1 - \sum_{k=1}^{p} \left(\rho_{j,k} - \bar{\rho}_i\right)^2\right)$ is strictly non-negative, we see that this inequality holds when

$$\sum_{k=1}^{p} \left(\rho_{j,k} - \bar{\rho}_i\right)^2 < 1$$

Thus, we have a more efficient estimator of $\delta$ when

$$p > \frac{1}{Var\left(\rho_{j,k}\right)}$$

In practice, we typically have a large number of genes, $p$, so that our transition matrix estimator will be expected to be dramatically more efficient than the commonly used Pearson or WGCNA estimators.

# References

[1] Jeremiah J Faith, Boris Hayete, Joshua T Thaden, Ilaria Mogno, Jamey Wierzbowski, Guillaume Cottarel, Simon Kasif, James J Collins, and Timothy S Gardner. Large-scale mapping and validation of escherichia coli transcriptional regulation from a compendium of expression profiles. *PLoS Biol*, 5(1):e8, 2007.

[2] Brendan J Frey and Delbert Dueck. Clustering by passing messages between data points. *science*, 315(5814):972–976, 2007.

[3] Kimberly Glass, Curtis Huttenhower, John Quackenbush, and Guo-Cheng Yuan. Passing messages between biological networks to refine predicted interactions. *PloS one*, 8(5):e64832, 2013.

[4] Kimberly Glass, John Quackenbush, Edwin K Silverman, Bartolome Celli, Stephen I Rennard, Guo-Cheng Yuan, and Dawn L DeMeo. Sexually-dimorphic targeting of functionally-related genes in copd. *BMC systems biology*, 8(1):118, 2014.

[5] Kimberly Glass, John Quackenbush, Dimitrios Spentzos, Benjamin Haibe-Kains, and Guo-Cheng Yuan. A network model for angiogenesis in ovarian cancer. *BMC bioinformatics*, 16(1):115, 2015.

[6] Peter Langfelder and Steve Horvath. Wgcna: an r package for weighted correlation network analysis. *BMC Bioinformatics*, (1):559, 2008.

[7] Peter Langfelder and Steve Horvath. Fast R functions for robust correlations and hierarchical clustering. *Journal of Statistical Software*, 46(11):1–17, 2012.

[8] Taotao Lao, Kimberly Glass, Weiliang Qiu, Francesca Polverino, Kushagra Gupta, Jarrett Morrow, John Dominic Mancini, Linh Vuong, Mark A Perrella, Craig P Hersh, et al. Genome medicine. 2015.

[9] Michael Levine and Robert Tjian. Transcription regulation and animal diversity. *Nature*, 424(6945):147–151, 2003.

[10] Adam A Margolin, Ilya Nemenman, Katia Basso, Chris Wiggins, Gustavo Stolovitzky, Riccardo D Favera, and Andrea Califano. Aracne: an algorithm for the reconstruction of gene regulatory networks in a mammalian cellular context. *BMC bioinformatics*, 7(Suppl 1):S7, 2006.

[11] Catharina Olsen, Kathleen Fleming, Niall Prendergast, Renee Rubio, Frank Emmert-Streib, Gianluca Bontempi, Benjamin Haibe-Kains, and John Quackenbush. Inference and validation of predictive gene networks from biomedical literature and gene expression data. *Genomics*, 103(5):329–336, 2014.

[12] Timothy Ravasi, Harukazu Suzuki, Carlo Vittorio Cannistraci, Shintaro Katayama, Vladimir B Bajic, Kai Tan, Altuna Akalin, Sebastian Schmeier, Mutsumi Kanamori-Katayama, Nicolas Bertin, et al. An atlas of combinatorial transcriptional regulation in mouse and man. *Cell*, 140(5):744–752, 2010.

[13] Erzsébet Ravasz, Anna Lisa Somera, Dale A Mongru, Zoltán N Oltvai, and A-L Barabási. Hierarchical organization of modularity in metabolic networks. *science*, 297(5586):1551–1555, 2002.
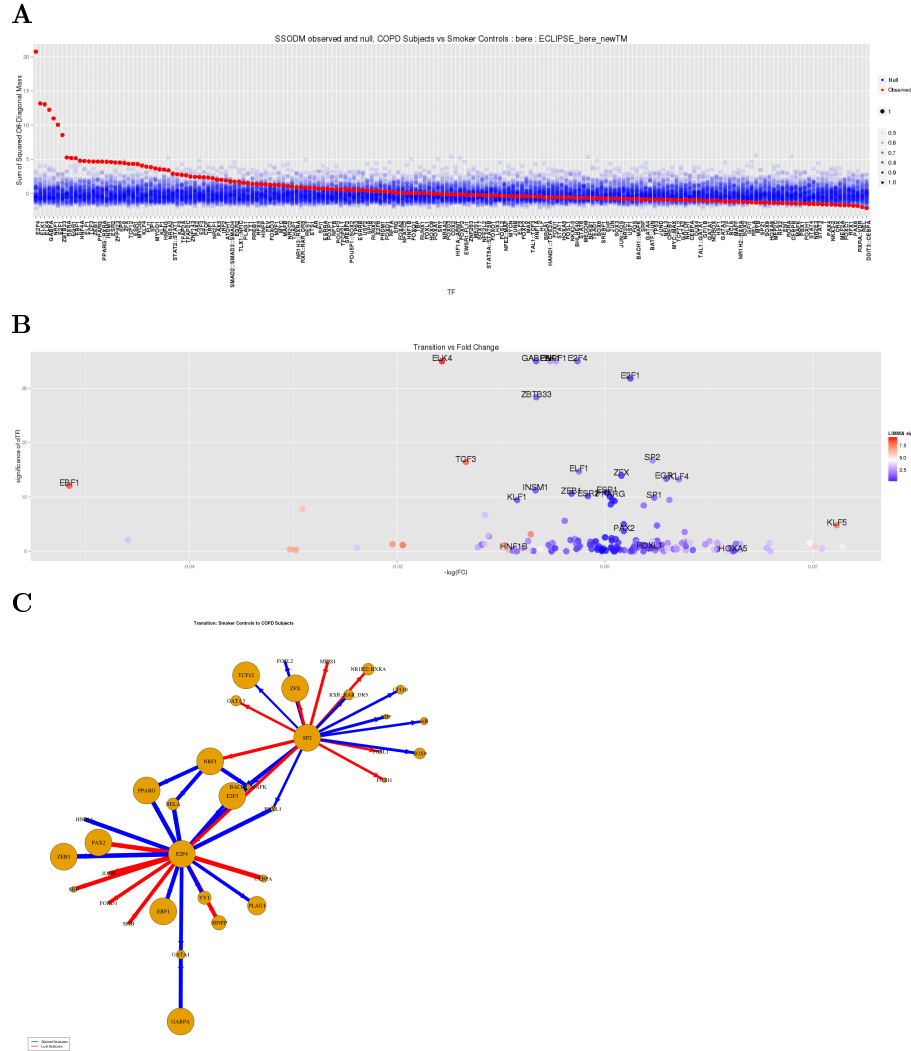
**A**



**B**



**C**



Figure 4: **(A)** Differential transcription factor involvement for the observed case-control (red) scaled for each TF by the distribution under the randomized case-control. **(B) Comparison of TF differential involvement vs differential expression.** TFs which are differentially involved are not necessarily differentially expressed and vice versa. Many TFs can be observed which have significantly different targetting patterns, but which are not statistically significantly differentially expressed. This suggests that our method finds transcription factors which are differentially affected at a post-transcription stage. **(C) Driver network transitions**. Network transitions are depicted here with arrows indicating the flow of targetting patterns from one transcription factor to another. Edges are sized according to the magnitude of the transition and nodes (TFs) are sized by the overall dTFI for each TF. The gain of targetting features is indicated by the color blue while the loss of features is indicated by red.
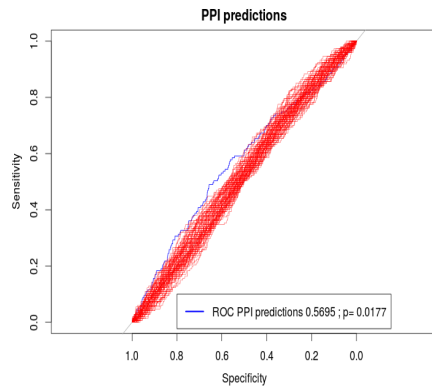
16

Figure 5: ROC curve for prediction of PPI based on a transition from Smoker control to COPD (blue) compared to a random case-control partition of the ECLIPSE data.